CHEMISTRY
A EUROPEAN JOURNAL

DOI: 10.1002/chem.200600109

Competing Magnetic Interactions in $Na_{10}Co_4O_{10}$, Studied by Neutron Diffraction

Norbert Stüßer,[b] Mikhail Sofin,[a] Roland Bircher,[c] Hans-Ulrich Güdel,[c] and Martin Jansen*[a]

Abstract: $Na_{10}Co_4O_{10}$ was investigated by neutron powder diffraction at 230, 70, and 4 K. The crystal structure, determined previously by X-ray diffraction on single crystals, was confirmed. $Na_{10}Co_4O_{10}$ orders magnetically below 37 K. All observed magnetic reflections could be indexed by integers (*hkl*) with respect to the chemical unit cell and the magnetic propagation vector $q=0$. The refinement was performed in the Shubnikov space group *C*2/*c* and indicated a collinear antiferromagnetic spin structure. The determined spin arrangement is consistent with the magnetic intratetramer interactions suggested previously from the analysis of magnetic susceptibility data: the magnetic moments of the central Co^{III} ions of the Co_4O_{10} tetramer lie parallel to each other and couple in an antiparallel fashion to the terminal Co^{II} moments. The Rietveld analysis shows that the net moments of 0.64 μ_B per tetramer form ferromagnetic layers parallel to the *ab* plane. Adjacent layers are coupled antiferromagnetically along *c*. The spins are aligned in the *ac* plane along the line connecting adjacent Co^{II} and Co^{III} ions of the tetramer. We have determined unusually low values for the ordered magnetic moments of 2.43(5) μ_B and 2.11(6) μ_B for Co^{III} and Co^{II}, respectively. The occurrence of spontaneous magnetization below 37 K indicates a slight canting of 2.2° of the antiferromagnetic structure. A representation analysis shows that a weak ferromagnetic component along *b* is compatible with the determined antiferromagnetic structure.

Keywords: cobalt · magnetic structure · mixed-valent compounds · oxo ligands

Introduction

Single molecular magnets[1] are currently attracting a great deal of attention because of spectacular quantum phenomena observed by microscopic methods. For practical applications a large overall magnetic moment of a singular cluster as well as a strong magnetic exchange of interacting centers are desirable. The former requirement can be satisfied in a simple case by involving magnetic centers with large moments. Thus typical single molecular magnets are composed from 3d transition ions and organic or inorganic bridging and coordinating ligands. Unfortunately, for all known single molecular magnets the quantum phenomena can be observed only at low temperatures (<10 K) since the coupling strengths are not strong enough in comparison to thermal energies at ambient conditions. If one wants to introduce intercluster interactions and to study their impact on the phenomena mentioned, in particular, the competition between intra- und intercluster interactions, one has to switch to chemical systems in which the clusters are less effectively isolated and insulated by organic ligands. Alkali oxometalates of the transition elements consisting of oligomeric complex oxoanions, which contain magnetic centers of diverse spin moments, would match these requirements. Recently, we succeeded in obtaining a novel sodium oxocobaltate,[2] which contains the tetrameric mixed-valent Co_4O_{10} anion. Its magnetic properties are rather unusual; it shows significant magnetic exchange interactions already at room temperature (see Figure 1). The temperature dependence of χ can be rationalized by assuming strong antiferromagnetic intracluster exchange interactions between Co^{II} and Co^{III} ions dominating the high-temperature magnetic behavior.

[a] Dr. M. Sofin, Prof. Dr. M. Jansen
Max-Planck-Institut für Festkörperforschung
Heisenbergstrasse 1, 70569 Stuttgart (Germany)
Fax: (+49) 711-689-1502
E-mail: m.jansen@fkf.mpg.de

[b] Dr. N. Stüßer
Hahn-Meitner-Institut
Glienicker Strasse 100, 14109 Berlin (Germany)

[c] Dipl. Chem. R. Bircher, Prof. Dr. H.-U. Güdel
Department of Chemistry and Biochemistry
University of Bern
Freiestrasse 3, 3000 Bern 9 (Switzerland)

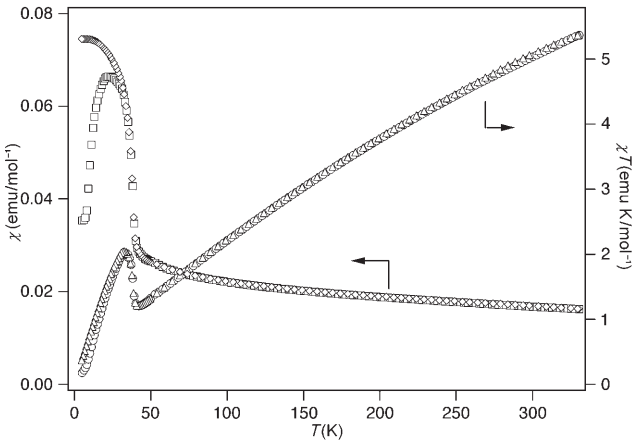

Figure 1. Magnetic susceptibility of $Na_{10}Co_4O_{10}$ represented as χ versus T and χT versus T, ZFC (□, ○) and FC (◇, △), respectively.

Below 38 K intercluster interactions become important and lead to cooperative effects. The interaction between the central Co^{III} ions is much weaker, and could be roughly quantified only in an indirect way through measurements on $Na_6Co_2O_6$[3] where a virtually identical surrounding of Co^{3+} ions is observed. To extend and corroborate that explanation, in this work we present our investigations on the magnetic structure of $Na_{10}Co_4O_{10}$ obtained by neutron diffraction, which in particular shed light on the role of intra- and intercluster interactions in the magnetic properties of transition metal oxides.

Experimental Section

Polycrystalline samples of $Na_{10}Co_4O_{10}$ ($\approx$5 g) were obtained by the azide/nitrate route[4] through procedures described in our previous papers.[2,5] The powder was placed into a cylindrical vanadium container and loaded into a standard helium flow cryostat. Neutron diffraction measurements were done with the D2B (high resolution) and D20 (high flux) powder diffractometers at the ILL in Grenoble. The high intensity mode was used at D2B to collect data at 230, 70, and 4 K, the wavelength was 1.594 Å. Data sets cover a range in 2θ up to 160° and have an angular resolution of 0.05°. The temperature dependence of the magnetic Bragg reflections was measured on the instrument D20. The Rietveld method[6] was used to refine the crystal and magnetic structure. The analysis of the data was performed by using the FullProf package.[7,8] The magnetic structure was drawn with Atoms.[9]

Results

Chemical structure: The neutron powder diffraction data collected at 300 and 70 K were used to refine the chemical structure in the space group $C2/c$. In total 59 parameters were refined with respect to the $Na_{10}Co_4O_{10}$ phase. These are 10 profile parameters for scale, lattice constants a, b, c, and β, half-width parameters U, V, W, one profile shape parameter and at lower diffraction angles two parameters accounting for asymmetries in the line shape. The remaining 48 parameters determine the three fractional coordinates and one isotropic temperature factor for each of the 12 sites. The occupancy factors were all fixed to one. A fraction of about 2 % (weight) of $NaCoO_2$ (space group $R\bar{3}$) was determined by simultaneously refining a second phase. The background was calculated by linear interpolation between given points. Table 1 and Table 2 list the relevant structural parameters determined from the 230 K data together with the residuals indicating the quality of the fit. All fits agree very well with the collected data confirming former analyses of X-ray diffraction patterns. The data collected at 70 K were treated in a similar way and the results were consistent with those from the 230 K data set. Figure 2, which shows the Rietveld fit using the data collected at 230 K, allows a visualization of the quality of the refinement.

Table 1. Lattice parameters and residuals of corresponding refinements for $Na_{10}Co_4O_{10}$.

	230 K	70 K	4 K
space group		$C2/c$	
a [Å]	14.8697(4)	14.8527(4)	14.8524(4)
b [Å]	8.0791(2)	8.0639(2)	8.0630(2)
c [Å]	11.3955(3)	11.3809(3)	11.3810(3)
β [°]	104.639(2)	104.693(2)	104.640(2)
cell volume [Å^3]	1324.55(6)	1318.52(6)	1318.32(5)
R_p [%]	7.90	7.03	6.13
R_{wp} [%]	8.52	7.81	6.65
R_{Bragg} [%]	3.78	2.97	2.79
χ^2	1.20	1.21	0.74

Table 2. Atomic parameters for $Na_{10}Co_4O_{10}$ at 230 K. The thermal parameter B is defined by the temperature factor $\exp\{-Bq^2/2\}$ with q the reciprocal lattice vector.

Atom	x	y	z	B_{iso}
Co1	0.2616(6)	0.8829(13)	0.2292(7)	1.03(13)
Co2	0.0485(5)	0.8657(11)	0.0584(7)	0.91(14)
Na1	0.9886(4)	0.6066(8)	0.8760(4)	1.27(10)
Na2	0.1055(4)	0.6693(7)	0.2904(5)	1.15(10)
Na3	0.1065(4)	0.9075(7)	0.8090(5)	0.88(9)
Na4	0.1621(5)	0.1663(8)	0.0371(6)	1.57(12)
Na5	0.1978(4)	0.5927(7)	0.0184(5)	1.37(11)
O1	0.0192(3)	0.0804(4)	0.1072(3)	1.48(8)
O2	0.3745(2)	0.8885(5)	0.1929(3)	0.92(6)
O3	0.1747(3)	0.8660(5)	0.0750(3)	1.11(7)
O4	0.2230(3)	0.8731(5)	0.3672(3)	1.29(5)
O5	0.9958(3)	0.6792(4)	0.0902(4)	1.46(7)

Magnetic structure: The prominent structural feature is the tetrameric oxoanion (Figure 3). Within this unit there are two edge-sharing tetrahedra to which two CoO_3 triangles are attached, through one vertex each. The observed magnetic reflections could be indexed by integers (hkl) with respect to the chemical unit cell, and the magnetic propaga-

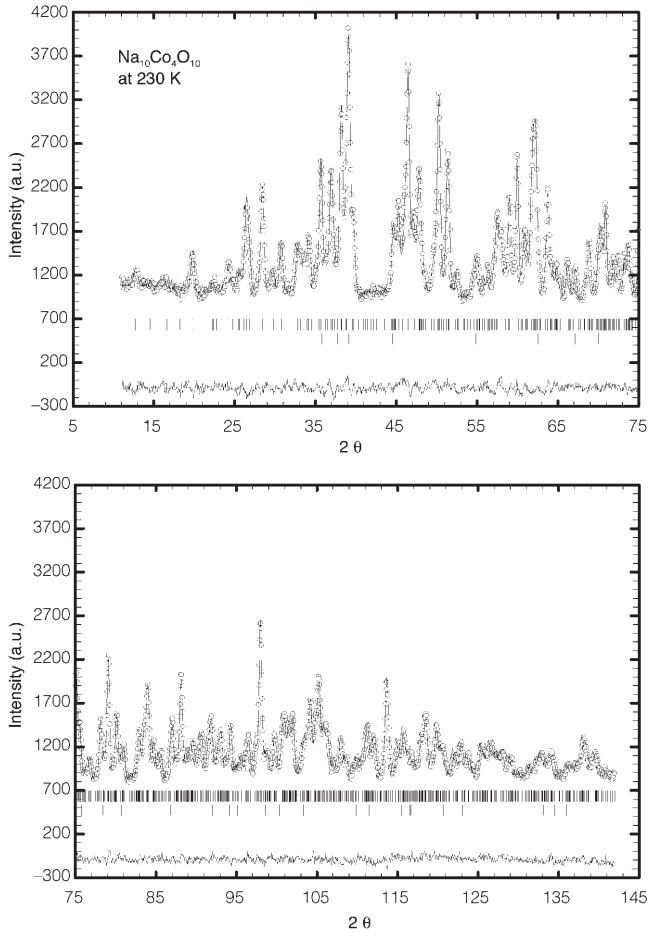

Figure 2. Experimental (circles) and calculated (full line) neutron powder diffraction pattern including difference plot (lower part) of $Na_{10}Co_4O_{10}$ measured at 230 K. Bragg positions of the nuclear reflections are indicated by bars. The second row of bars marks reflection positions for the $NaCoO_2$ impurity.

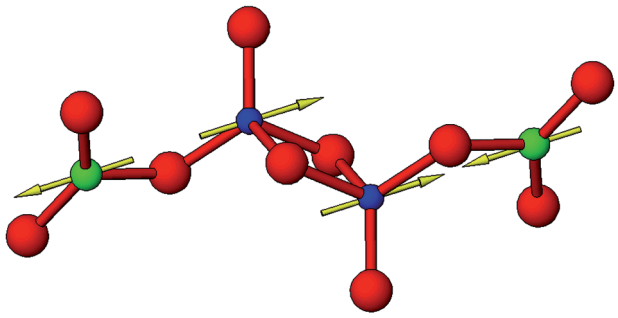

Figure 3. Structure of magnetic moments within the Co_4O_{10} oligomer.

tion vector becomes $q=0$. The clear and strong presence of the (001) reflection and the absence of the (100) and (010) reflections limit the possible spin arrangements. The Co^{III} ions are located at $z=0.05$ and 0.95 or at $z=0.45$ and 0.55, while the Co^{II} ions are positioned at $z=0.2$ and 0.3 as well as at $z=0.7$ and 0.8. Thus, overall there are planes at $z\approx0$ and 0.5 occupied by Co^{III} and planes at $z\approx0.25$ and 0.75 occupied by Co^{II}. It should be noted that the two central Co^{III} ions of one oxoanion are located on the same z plane. A ferromagnetic coupling of the spins of the Co^{III} ions as suggested in reference [2] is strongly indicated, because an antiferromagnetic arrangement of these spins would give rise to a zero net moment on the Co^{III} planes so that mainly the Co^{II} spins could contribute to the (001) reflection. For the latter only one spin arrangement is possible with a (001) reflection and no intensity at (100) and (010). This spin order, however, does not reproduce satisfactorily the observed pattern and has to be ruled out. The appearance of the (001) reflection suggests that all Co^{III} ions located close to $z=0$ have moments parallel to each other, while those located around $z=0.5$ have a moment in the opposite direction. This fixes all mutual spin orientations of Co^{III} ions within the chemical unit cell. However, the coupling between Co^{III} and Co^{II} remains open. Refinements were performed with two models for the magnetic structure. In the first model we used the spin configuration for the Co^{III} introduced above and the antiferromagnetic coupling between Co^{II} and Co^{III}. In the second model this latter coupling was chosen to be ferromagnetic. Refinements were done simultaneously for the chemical and the magnetic structure. Initially, all three components of the moments for both Co^{II} and Co^{III} were refined independently. The first model gives an excellent agreement between the calculated and the measured powder pattern, whereas the second could not describe the experimental data at all. It turned out from the refinements using the first model that the y component of the moments was very low and could be fixed to zero within the error. Moreover the refinements indicated approximately a collinear spin structure. Finally, the moments were constrained to the *ac* plane, which allowed only a collinear structure. The refinement is shown in Figure 4 and the results are listed in Tables 1, 3, and 4. The obtained spin arrangement is invariant under the magnetic space group $C2/c$. The intratetramer spin arrangement is shown in Figure 3 and the intertetramer couplings of the net moments inside the unit cell are displayed in Figure 5. The latter couplings are ferromagnetic in the *ab* plane. Adjacent planes order antiferromagnetically. Furthermore we have looked at the temperature behavior of the magnetic structure. No indication was found for further magnetic phase transitions. In Figure 6 we show the temperature variation of the reduced sublattice magnetization M/M_0. The latter was determined from the magnetic Bragg peak intensity I_m using $M/M_0=(I_m/I_0)^{1/2}$ with I_0 taken as the magnetic Bragg intensity at 4 K. The data are consistent with a continuous second-order phase transition. An analysis of the critical behavior turned out to be unsatisfactory due to the insufficient amount of data and statistics close to the transition point. One can estimate from the data that the transition temperature is around 38 K.

Discussion

First we will consider the spin arrangement within the tetramer. The magnetic structure indicates antiferromagnetic

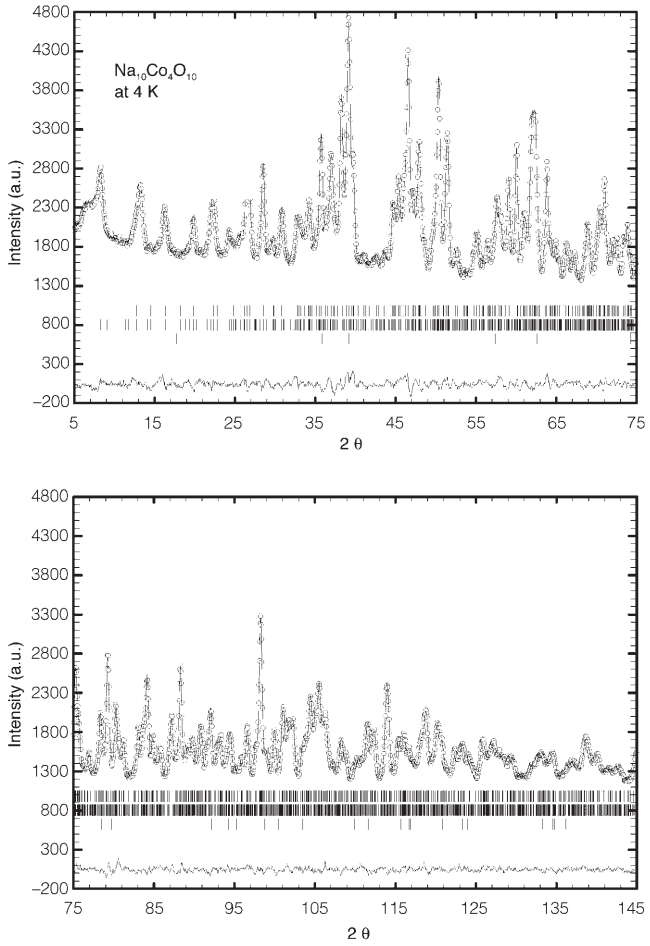

Figure 4. Experimental (circles) and calculated (full line) neutron powder diffraction pattern including difference plot (lower part) of $Na_{10}Co_4O_{10}$ measured at 4 K. Bragg positions of the nuclear and magnetic reflections are indicated by the first and second row of bars, respectively. The last row belongs to the $NaCoO_2$ impurity.

Table 3. Atomic parameters for $Na_{10}Co_4O_{10}$ at 4 K. See Table 2 for definition of B.

Atom	x	y	z	B_{iso}
Co1	0.2643(4)	0.8836(9)	0.2296(5)	0.18(10)
Co2	0.0490(4)	0.8640(8)	0.0574(5)	0.34(10)
Na1	0.9890(3)	0.6073(7)	0.8737(4)	0.73(8)
Na2	0.1053(4)	0.6710(6)	0.2899(5)	1.13(9)
Na3	0.1072(3)	0.9049(5)	0.8088(4)	0.42(7)
Na4	0.1629(4)	0.1668(6)	0.0383(4)	0.91(9)
Na5	0.1991(3)	0.5921(7)	0.0172(4)	0.92(8)
O1	0.0200(2)	0.0801(4)	0.1084(3)	0.93(6)
O2	0.3746(2)	0.8863(4)	0.1911(3)	0.69(5)
O3	0.1747(2)	0.8657(5)	0.0741(3)	0.65(6)
O4	0.2224(2)	0.8718(4)	0.3671(3)	0.91(5)
O5	0.9959(2)	0.6788(3)	0.0897(3)	0.62(5)

Table 4. Magnetic moments obtained from refinement with a residual $R_m = 5.02$ at 4 K. Spherical coordinates θ and ϕ indicate orientation of moment with respect to the y axis and x axis, respectively.

Site/Moments [μ_B]	$\lvert M \rvert$	ϕ	θ	M_x	M_y	M_z
Co1	2.11(6)	63.6(8)°	90°	1.95(6)	0	1.43(4)
Co2	−2.43(5)	63.6(8)°	90°	−2.25(4)	0	−1.65(5)

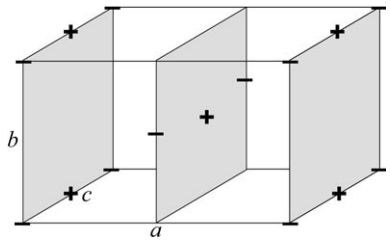

Figure 5. Arrangement of the net spins per tetramer within one unit cell. Each symbol + or − denotes orientation of the net spin of the tetramer.

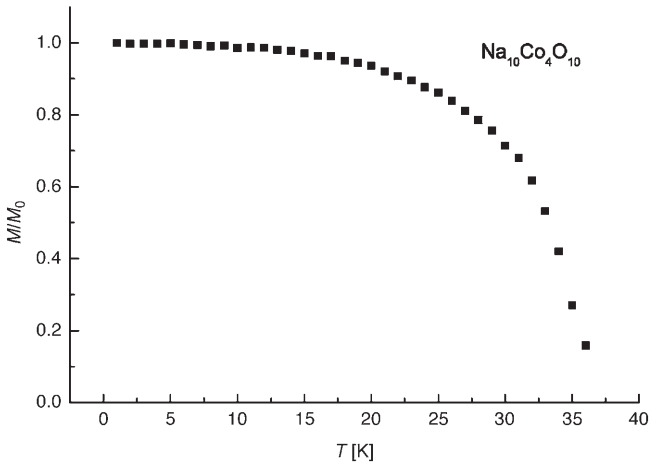

Figure 6. Reduced magnetization as a function of temperature, derived from magnetic Bragg intensities at (1 −2 0) using $M/M_0 = (I_m/I_0)^{1/2}$.

coupling between Co^{II} and Co^{III} within one tetramer. This supports earlier results obtained from the analysis of susceptibility data which are discussed in reference [2]. There, a strong antiferromagnetic Co^{II}–Co^{III} superexchange interaction was suggested and a model fit to the data yielded a coupling strength of $2J = -81\ cm^{-1}$. Furthermore, our present analysis shows a ferromagnetic spin alignment between the central Co^{III} ions. This coupling is expected to be weaker[2] and a susceptibility study on $Na_6Co_2O_6$,[3] which contains Co_2O_6 dimers that are exactly the inner parts of the tetramers, has confirmed that.

To understand the three-dimensional magnetic ordering below 38 K one has to take into account superexchange paths at longer distances. A coupling of Co^{II}–Co^{II} with an interatomic distance of 4.1 Å along b could be possible, which would give rise to ordered magnetic chains or even planes if a weak ferromagnetic intratretamer Co^{III}–Co^{III} interaction becomes active. To form the three-dimensional magnetic lattice, a coupling of Co ions belonging to different planes has to be present as well, like, for example, the one between Co^{III} ions, having a path directed along c with a distance of 4.9 Å. It should be noted that the three-dimensional order can be established by crossover behavior in the presence of weak interactions.[10] Since crossovers are driven by the divergence of the correlation length in the low-dimensional

system at least one intertetramer coupling has to be of significant strength to cause long-range order around 37 K.

Let us finally try to determine the mechanism by which the magnetic coupling between the tetramers and thus the long-range magnetic order is induced. Of the two principal candidates, exchange interactions and magnetic dipole–dipole interactions, the latter can be quantitatively estimated. Placing a $S=1$ spin at the centers of a pair of nearest-neighbor tetramers and using the formula given in Equation (1)[12]

$$E_{\mathrm{dip}} = \frac{\mu_0}{4\pi}\frac{g^2{\mu_{\mathrm{B}}}^2 S^2}{r^3} \qquad (1)$$

we obtain an interaction energy $E_{\mathrm{dip}}=0.01\ \mathrm{cm}^{-1}$. Inserting this into the mean field formula given in Equation (2)[13]

$$T_{\mathrm{c}} = \frac{S(S+1)zE_{\mathrm{dip}}}{3k_{\mathrm{B}}}$$

with $z=8$ being the number of neighboring tetramers, yields an ordering temperature of 0.07 K. Even considering the very approximate nature of this estimate, magnetic dipole–dipole interactions can clearly be ruled out as the driving mechanism for the magnetic order. This leaves exchange interactions. The shortest Co^{2+}–Co^{2+} distance between adjacent tetramers in $Na_{10}Co_4O_{10}$ is 4.1 Å along the b axis. This is a very close approach, and either direct or superexchange antiferromagnetic interactions of the order of a few cm^{-1} could result. In a mean-field model a J_{inter} of $-5\ \mathrm{cm}^{-1}$ between the tetramers is required to lead to a three-dimensional ordering temperature of 37 K.

Next we will shortly discuss the sizes of the ordered moment of 2.11 μ_B and 2.43 μ_B, which have been determined for Co^{II} and Co^{III}, respectively. Both values are well below the values of 3 μ_B and 4 μ_B, respectively, expected for a spin-only moment for the isolated ions. This could be related to an ordered magnetic state in which the moments are not fully ordered at low temperature. This view may be supported by the observed difference between the field-cooled (fc) and zero-field-cooled (zfc) susceptibility.[2] The qualitative temperature behavior of the susceptibility in the ordered state below 37 K shows some resemblance with that of spin glasses.[11] In the latter the fc susceptibility stays nearly constant and is well above χ_{zfc}. One could speculate that the reduced ordered moment is attributed to the occurrence of frustration among the exchanges.

A comparison of the results obtained here by neutron diffraction with those derived previously from magnetic[2] and calorimetric measurements is very revealing. In Figure 7 we show the results of magnetic and heat capacity measurements on a polycrystalline sample of the title compound below 50 K. We have the clear signature of a magnetic ordering transition at (37±1) K. The similarity to Figure 6, in which the sublattice magnetization is plotted, clearly indicates that all the three discontinuities are the result of three-dimensional magnetic order. But the order determined

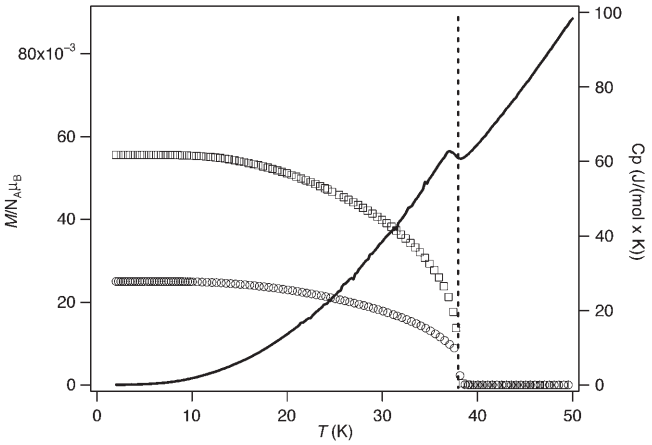

Figure 7. Heat capacity (solid line) and magnetic moment of $Na_{10}Co_4O_{10}$ measured in an applied field of 7.7 G in field-cooled (squares) and zero-field-cooled (circles) measurement mode. The dotted line denotes the magnetic ordering temperature of (37±1) K.

by neutron diffraction is antiferromagnetic, whereas the magnetic data show a non-zero spontaneous magnetization. This apparent contradiction can be resolved by some quantitative considerations.

As pointed out above the intratetramer spin arrangement derived from high-temperature magnetic susceptibility measurements[2] is consistent with the finding from the magnetic neutron diffraction, and as a result the tetramer ground state of $Na_{10}Co_4O_{10}$ is $S=1$. However, the spontaneous magnetization below 37 K shown in Figure 7 and the observation of magnetic hysteresis at 4.5 K (not shown) are not compatible with the antiferromagnetic order. A quantitative analysis of the magnetic data obtained with the smallest external field of 7.7 G yields an ordered moment of $M=$ 0.0125 μ_B per tetramer. This is much smaller than the saturation moment $M_{\mathrm{sat}}=gS=2\ \mu_B$, calculated for a tetramer with $S=1$ and $g=2$. It is also much smaller than the ordered moment of 0.64 μ_B per tetramer determined for the magnetically ordered structure by neutron diffraction. This strongly indicates that we are dealing with a canted antiferromagnet, and based on the ordered moment of 0.64 μ_B per tetramer we calculate a canting angle of 2.2°. This canting is not accessible to magnetic diffraction by unpolarized neutrons.

It is now instructive to highlight the crystallographic symmetry with respect to the antiferromagnetic structure determined by neutron diffraction and the weak ferromagnetism observed in the magnetic measurements. We present here a short representation analysis as described in reference [14] for the case where the magnetic and chemical cells are identical. In the frame of this analysis the transformation behavior of the observed antiferromagnetic and ferromagnetic modes has to be associated with irreducible representations of the space group. In a first step we choose the 2_y rotation axis in (0, y, 1/4); the 2_{1y} screw axis in (1/4, y, 1/4); and a center of symmetry -1 in (0, 0, 0) as the generating symmetry elements of the space group $C2/c$. Table 5 lists the coordinates of the general Wyckoff position 8f and the Bravais

Table 5. Symmetry related coordinates for Wyckoff position 8*f* (IT) in *C*2/*c*. The observed af + − + − + − + − and − + − + − + − + modes for Co^{II} and Co^{III}, respectively will be denoted by $\boldsymbol{G}^{+}$ henceforth.

Bravais sublattices				Co^{II}	Co^{III}
1	x	y	z	+	−
2	$-x$	y	$-z+1/2$	−	+
3	$-x$	$-y$	$-z$	+	−
4	x	$-y$	$z+1/2$	−	+
5	$x+1/2$	$y+1/2$	z	+	−
6	$-x+1/2$	$y+1/2$	$-z+1/2$	−	+
7	$-x+1/2$	$-y+1/2$	$-z$	+	−
8	$x+1/2$	$-y+1/2$	$z+1/2$	−	+

sublattices are numbered by (1) to (8). The equations of transformation now become:

$2_y S_{ix,z} = S_{jx,z}$, with Bravais numbers $(i)(j) = (1)(2)$; (5)(6); (3)(4); (7)(8)

$2_y S_{iy} = S_{jy}$, with Bravais numbers $(i)(j) = (1)(2)$; (5)(6); (3)(4); (7)(8)

$2_{1y} S_{iy} = S_{jy}$, with Bravais numbers $(i)(j) = (1)(6)$; (2)(5); (3)(8); (4)(7)

$2_{1y} S_{ix,z} = S_{jx,z}$, with Bravais numbers $(i)(j) = (1)(6)$; (2)(5); (3)(8); (4)(7)

$1 S_{ix,y,z} = S_{jx,z}$, with Bravais numbers $(i)(j) = (1)(3)$; (2)(4); (5)(7); (6)(8)

The last two columns in Table 5 indicate the antiferromagnetic structure for Co^{II} and Co^{III} as obtained from our neutron diffraction data. Now one considers the transformation properties of the *x, y, z* components of the $\boldsymbol{G}^{+}$-labeled linear spin combination $\boldsymbol{G}^{+} = \boldsymbol{S_1 - S_2 + S_3 - S_4 + S_5 - S_6 + S_7 - S_8}$ corresponding to the found spin structure for Co^{II} and Co^{III} under the generating symmetry elements (e.g. $2_y G^{+}{}_{x} = G^{+}{}_{x}$). The results of these transformations for $G^{+}{}_{x}$, $G^{+}{}_{y}$, and $G^{+}{}_{z}$ are quoted in Table 6 together with the transformation behavior for the components of the ferromagnetic vector $\boldsymbol{F}^{+} = \boldsymbol{S_1 + S_2 + S_3 + S_4 + S_5 + S_6 + S_7 + S_8}$. These directly determine the associated irreducible representations, in our case $\Gamma_1(+\,+\,+)$ and $\Gamma_4(-\,-\,+)$. In the approximation of a magnetic hamiltonian of the order of two in terms of the spins, only products of base vectors belonging to the same representation are allowed to enter the hamiltonian as invariants. In our case $G^{+}{}_{x}$ can couple with $G^{+}{}_{z}$ and $F^{+}{}_{y}$ and no coupling is possible with another ferromagnetic component.

Table 6. Transformation properties of the base vectors of $\boldsymbol{G}^{+}$ and $\boldsymbol{F}^{+}$ modes.

				Basis vectors
	2_y	2_{1y}	-1	
representation				
Γ_1	+	+	+	$\boldsymbol{G^{+}_x, G^{+}_z, F^{+}_y}$
Γ_4	−	−	+	$\boldsymbol{G^{+}_y, F^{+}_x, F^{+}_z}$

Since our neutron diffraction analysis showed the presence of antiferromagnetic modes $G^{+}{}_{x}$ and $G^{+}{}_{z}$, only a ferromagnetic ordering along the *y* direction is possible.

Conclusion

In conclusion, our neutron powder diffraction experiments allowed us to determine the collinear three-dimensional long-range antiferromagnetic order in $Na_{10}Co_4O_{10}$. The intratetramer spin arrangement confirmed the results of former susceptibility measurements. The intertetramer couplings could be determined from the Rietveld refinement unambiguously. The ordered moments are well below the values for the corresponding free ions. The presence of a ferromagnetic component in the spin structure as observed in magnetization measurements is confirmed by a representation analysis of the magnetic structure. $Na_{10}Co_4O_{10}$ is very likely to possess weak ferromagnetism along *b* in addition to its basic antiferromagnetic structure with spins in the *ac* plane.

Acknowledgement

We thank O. Leynaud for his support during the experiments at ILL.

[1] G. Christou, D. Gatteschi, D. N. Hendrickson, R. Sessoli, *Mater. Res. Bull.* **2000**, *35*, 66.
[2] M. Sofin, H.-U. Güdel, R. Bircher, E.-M. Peters, M. Jansen, *Angew. Chem.* **2003**, *115*, 3651; *Angew. Chem. Int. Ed.* **2003**, *42*, 3527.
[3] M. Sofin, E.-M. Peters, M. Jansen, *J. Solid State Chem.* **2004**, *177*, 2550.
[4] D. Trinschek, M. Jansen, *Angew. Chem.* **1999**, *111*, 234; *Angew. Chem. Int. Ed.* **1999**, *38*, 133.
[5] M. Sofin, E.-M. Peters, M. Jansen, *Z. Anorg. Allg. Chem.* **2002**, *628*, 2691.
[6] H. M. Rietveld, *J. Appl. Crystallogr.* **1969**, *2*, 65.
[7] J. Rodriguez-Carvajal, Programm: FULLPROF 98, Version 0.2, Mar98-LLB JRC, Laboratoire Leon Brillouin (CEA-CNRS), France **1998**.
[8] J. Rodriguez-Carvajal, *Phys. B* **1993**, *192*, 55.
[9] Eric Dowty, Atoms, Version 5.0.7, **1999**.
[10] L. J. de Jongh, *Magnetic Properties of Layered Transition Metal Compounds*, Kluwer, Dordrecht, **1990**, pp. 19–33.
[11] S. Nagata, P. H. Keesom, H. R. Harrison, *Phys. Rev. B* **1979**, *19*, 1633.
[12] A. Bencini, D. Gatteschi, *EPR of Exchange Coupled Systems*, Springer, New York, **1989**, pp. 68–70; and A. Bencini, D. Gatteschi, *EPR of Exchange Coupled Systems*, Springer, New York, **1989**, pp. 100–106.
[13] R. L. Carlin, *Magnetochemistry*, Springer, Berlin, **1986**, p. 328.
[14] E. F. Bertaut, *Acta Crystallogr.* **1968**, *24*, 217.

Received: January 24, 2006
Published online: May 9, 2006

